

# OPTIMIZING NMR DATA ACQUISITION AND DATA PROCESSING PARAMETERS FOR TIGHT-GAS MONTNEY FORMATION OF WESTERN CANADA

Babak Salimifard<sup>1</sup>, Mike Dick<sup>2</sup>, Derrick Green<sup>2</sup>, Douglas W. Ruth<sup>1</sup>  
*1- University of Manitoba, 2- Green Imaging Technologies*

*This paper was prepared for presentation at the International Symposium of the Society of Core Analysts held in Vienna, Austria, 27 August – 1 September 2017*

## ABSTRACT

With the emergence of unconventional resources as viable sources of producible hydrocarbons, characterization techniques have been modified to accommodate the challenges faced by the complicated pore network and rock structure of such rocks. Nuclear Magnetic Resonance (NMR) is widely used for rock and fluid characterization in both laboratory and at downhole conditions. Proper design of test parameters and analysis of the acquired signal is crucial for proper characterization of the medium. In this study a 1.5” diameter plug of Montney Formation of Northern BC, Canada was used to optimize parameters such as echo spacing, number of echoes, acquisition delays, and number of scans (signal to noise ratios) to ensure data quality while minimizing run time, background signals were sought after to avoid being misinterpreted as micropores, and post-scan data processing was performed to avoid oversmoothing the decay curve.

This study shows that due to the fast relaxing nature of the Montney rock, shorter echo spacing (TE) is more desirable. Ringing effects and background noises are negligible at  $\tau$  (TE/2) of 50  $\mu$ s. At longer  $\tau$ s (200  $\mu$ s) up to 77 percent of micro pore volume is lost while  $T_{2m}$  increases by 130 percent. However, a long acquisition time (up to 1000 msec) should be applied to capture the fluid in the micro and macro fractures if fracture characterization is desired. NMR volume stabilizes at an acquisition time of 250 msec. Shorter acquisition times result in up to 11% loss in NMR volume at a  $\tau$  of 50  $\mu$ sec. Longer  $\tau$ s are less sensitive to shorter acquisition times. A recycle delay (RD) study indicates that micro and meso pores are not affected by short recycle delay times; however, a longer recycle delay results in a 44% increase in the macro pore volume. A smoothing parameter of 0.2 was achieved as the optimal smoothing parameter for the Montney rock and proved to generate stable pore size distributions and free-to-bound volume ratios even at low signal to noise (SNR) ratios. A separate study discusses the measurement error in NMR volume as a function of scan duration and finds that at short  $\tau$ s there's up to a 0.5ml reduction in NMR volume per hour of scan time due to heating and 0.1ml reduction per hour due to drying.

## INTRODUCTION

Nuclear Magnetic Resonance (NMR) has been used extensively over the past two decades to characterize petroleum reservoir rocks and fluids both in the laboratory and at downhole. NMR characterizes pore network and fluids by monitoring the relaxation rate of the hydrogen nuclei present in the saturating fluids of the porous formation [1,2]. High data quality and proper data processing are key to successful rock and fluid characterization in unconventional resources while small pores, high surface to volume ratios, presence of

heavy hydrocarbons, and presence of organic pores and ferromagnetic minerals make data acquisition and processing much more challenging than that of conventional rocks [3,4].

**THE MONTNEY FORMATION**

The Montney formation is described as a fluvial sedimentary basin deposited in an open shelf marine environment on the western margin of the North American shield during the Triassic period under arid, mid-latitudinal conditions [5,6]. In the subsurface the Montney Formation extends over 700 kilometers from northern British Columbia to central Alberta and has a thickness of 100 to 300 meters, with thickness and depth increasing from east to west [7]. The Montney Formation is generally characterized as a siltstone-dominated lithology containing abundant dolomitized carbonates and immature feldspars combined with variable amounts of fine-grained shale and clay minerals [6,7]. The Total Organic Carbon (TOC) content of the Montney ranges from 0.1% to 3.6%, with an average of 0.8%. In this study a 1.5” plug sample of the Montney from the gas rich region of Montney in Northern British Columbia, Canada, was scanned and processed to optimize NMR acquisition and processing parameters. XRD and TOC measurements as well as porosity and permeability tests were done on end-pieces of the sample. The results are shown in Figure 1 and Table 1.

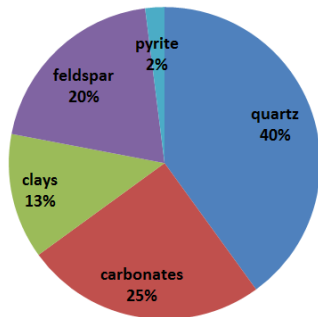


**Figure 1** – Summary of XRD results for A13UM1 end-pieces. Carbonates include 9% calcite,12.5% dolomite and 3% ankerite while present clays are only illite and mica.

**Table 1** – Summary of porosity, permeability and TOC measurements done on As-Received A13UM1 end-pieces

Well Location	b-070-C/094-A-13
Depth (m)	1855.80
Total Porosity (pu)	5.7
GRI Permeability (nD)	208
Grain Density (gr/ml)	2.71
Bulk Density (gr/ml)	2.56
TOC (%)	1.1

**THE CPMG PULSE SEQUENCE AND THE HARDWARE**

NMR signals are acquired using a series of pulse sequences consisting of radio frequency (rf) pulses and delay times. Choosing the optimal acquisition parameters requires an understanding of the pulse sequence. The Carr-Purcell-Meiboom-Gill (CPMG) pulse sequence is the most popular pulse sequence used for T<sub>2</sub> measurements. CPMG is initiated with a 90° pulse to align the magnetization vector in the xy-plane. After the pulse is turned off, the net magnetization vector disperses as some nuclei with higher Larmor frequency move faster and those with lower Larmor frequency lag behind. To re-phase all the spins a number of 180° pulses (echoes) are applied at specific time periods called “echo spacings” (TE). These pulses flip the spins to the other side of the xy-plane. As a result, nuclei with higher Larmor frequency would fall behind the ones with lower Larmor frequency and would eventually catch up to the slower ones and a rise in the magnetization vector is observed as the nuclei realign. Peak magnetization at each echo is captured as the echo

train and is the raw data for  $T_2$  distributions [8,9]. A schematic of the CPMG pulse sequence is shown in Figure 2.

A low-field Oxford Instruments bench-top rock analyzer with a  $B_0 = 0.3$  T permanent magnet was used in this study. The rf probe's dimensions are 60 mm long and 40 mm in diameter. Magnet temperature was stable at 35°C and typical 90° and 180° pulse durations are 10 and 20  $\mu$ s respectively which in combination with recovery time and group delays allows for a minimum CPMG echo time of 50  $\mu$ s. In this study, all scans were taken at a TE of 100  $\mu$ s, SNR of 100, RD time of 1000 ms and 10000 number of echoes (acquisition time of 1000 ms) using a 125 KHz digital filter, unless otherwise indicated.

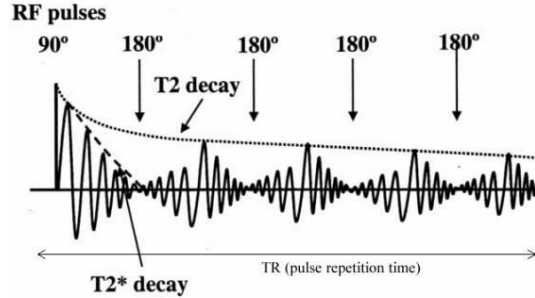


Figure 2 – A sample schematic of the CPMG pulse sequence.

## PROCESSING THE NMR SIGNAL

Raw CPMG data is measured as voltage decay versus time in an NMR tool. This decay, in a perfectly homogenous magnetic field, is the result of relaxation of the spins away from the  $xy$ -plane into their equilibrium state. This curve is then fitted with an exponential decay function to produce the commonly-used  $T_2$  distribution curve. In a porous medium, fluids in different pores relax at different rates; therefore a single exponential function cannot typically be used to fit the decay curve [10]. Assuming that there are  $n$  echoes, each with a magnitude  $g_i$  measured at  $t_i$ , the following equation in the form of a summation is used to fit the decay curve and minimize the error [11]:

$$g_i = \frac{M(t_i)}{M_0} = \sum_{j=1}^m a_j f_j e^{\frac{-t_i}{T_j}} + \epsilon_i \quad i=1,2,\dots,n \quad (\text{Eq. 1})$$

Here there are  $m$  known relaxation times,  $T_j$ , that are preselected to be equally spaced on the logarithmic scale.  $M(t_i)$  is the magnetization of the system at each  $t_i$  and  $M_0$  is the magnetization at  $t=0$ . The polarization factor,  $a_j$ , is defined as a function of Repeat-Delay (RD) time (the time between successive CPMG sequences) and is typically set to be one if long enough RD times are used. If shorter RD times are used,  $a_j$  can be given by

$$a_j = 1 - e^{-RD/T_{1j}} \quad (\text{Eq. 2})$$

$f_j$  is the frequency (incremental porosity) of the pores with a  $T_2$  relaxation of  $T_j$ , and  $\epsilon_i$  is the error. Eq. 1 is typically solved using non-negative least square regression on predefined  $T_2$  bins. Such solvers find the particular distribution that minimizes the deviation between the fit and the data with its random noise. As a result, they tend to generate sharp delta-function-like spikes at different  $T_j$  values which does not represent the continuous distribution of pore sizes in a porous medium. Also, because the inversion is highly affected

by the noise, the resulting distribution is not repeatable due to the random nature of the noise. To produce a repeatable  $f_j$  function, a penalty or regularization function is added to the solution. Although various types of penalty functions have been developed, a general form of regularization is shown here:

$$\varphi(f) = \frac{1}{2} \sum_{i=1}^n \left( \sum_{j=1}^m f_j e^{\frac{-t_i}{T_j}} - g_i \right)^2 + \alpha R(f_j) \quad (\text{Eq. 3})$$

where  $R(f_j)$  is the penalty function and  $\alpha$  is the smoothing parameter. The smoothing parameter should be adjusted in a way to avoid over-weighting the regularization function while producing stable peaks. Using a large  $\alpha$  will increase the weight of the regularization function and produce an over-smooth  $T_2$  distribution. Different Techniques exist to optimize  $\alpha$  to be commensurate with the measurement error. In this study BRD, T1-Heel, Full Span and GIT regularization techniques [12] are compared with a fixed smoothing parameter technique (Fixed  $\alpha$ ). The fixed smoothing parameter was obtained by scanning the sample at different saturations levels. The sample was initially scanned dry. Then it was placed in 2% KCl for 24 hours to imbibe brine. The sample was weighed at both stages and imbibed brine volume was calculated based on a brine density of 1.02 gr/ml (Table 2). The partially saturated sample was scanned and then both the dry and partially saturated NMR decay curves were converted to  $T_2$  relaxation distributions using smoothing parameters ranging from 0 to 1. At each smoothing parameter, the difference between partially saturated ( $V_i$ ) and dry ( $V_d$ ) NMR volumes ( $\Delta V_{NMR}$ )(Gray Trace Figure 3-a) was monitored and compared with the volume of the imbibed brine. An optimal smoothing parameter was selected where  $\Delta V_{NMR}$  matched the volume of imbibed brine. Table 2 and Figure 3 summarize the smoothing optimization process.

**Table 2** - Dry and Partially Saturated masses of the sample and calculated brine volume that was imbibed into the sample based on a brine density of 1.02 g/ml

Sample	Dry Mass (gr)	Mass After Imbibition (gr)	Brine Volume Imbibed (ml)
A13UM1	97.243	97.862	0.607

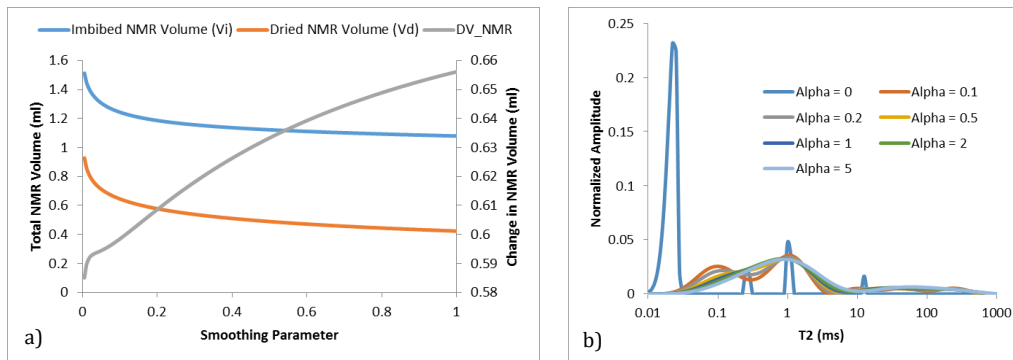


**Figure 3 - a)** NMR volume at dry and partially saturated (imbibed) using a series of smoothing parameters. The gray line represents the difference between the imbibed and dry volumes at each smoothing parameter.  $\Delta V_{NMR}$  matches the imbibed brine volume when the smoothing parameter is roughly 0.2. **b)** Normalized  $T_2$  distribution curve produced using different smoothing parameters. Very small smoothing parameters tend to produce unstable sharp peaks while large smoothing parameters tend to oversmooth the  $T_2$  distribution.

Figure 4 compares  $T_2$  relaxation times derived using each regularization technique. Figure 4 suggests that the T1-Heel and Full Span techniques tend to undersmooth the decay curve

and generate spiky  $T_2$  distributions while the GIT technique oversmooths the decay curve. The BRD technique creates comparable  $T_2$  distributions with distributions created using the fixed smoothing parameter. The BRD and Fixed  $\alpha$  techniques both generate stable distributions and produce similar total NMR volumes while T1-Heel and Full Span overestimate the total NMR volume. GIT's technique generates comparable NMR volume with that of BRD and Fixed  $\alpha$  despite oversmoothing the decay curve. Because the T1-Heel and Full Span smoothing techniques could not generate acceptable  $T_2$  distributions, they were excluded from further analysis.

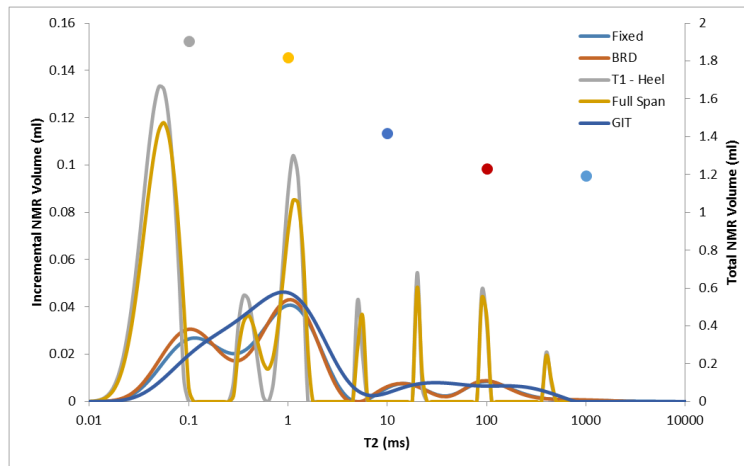


**Figure 4** – A comparison of different  $T_2$  distributions using five different regularization techniques. Solid dots represent the total NMR volume calculated using each technique.

## SIGNAL TO NOISE RATIO

Although the highest quality data is always desirable, NMR tests are routinely performed at low signal to noise ratios (SNR) to save time. SNR is the ratio of the initial magnitude of the echo train data to the noise amplitude and can be increased by increasing the number of successive scans. SNR would increase by a factor of  $\sqrt{2}$  per doubling the number of experiments. The optimal regularization technique should be able to not only produce reliable distributions at high SNR, but also be stable and produce reliable distributions at low SNR. In this study the sample used earlier was scanned at different SNRs. Fixed  $\alpha$ , GIT's and BRD regularization techniques were then used to produce  $T_2$  distributions. The tail of the  $T_2$  distribution curve ( $T_2$  larger than 4.5 ms) was taken as the signal coming from micro fractures and was not considered as the in-situ pore network of the rock.

Results (Figure 5 – panel (c)) show that Fixed  $\alpha$  is able to produce bi-modal distributions even at low SNR while NMR volume stabilizes at SNR of 57. GIT's technique (Figure 5 – panel (a)) produces unimodal distributions even at high SNR (excluding micro-fractures) while showing high stability both in  $T_2$  distribution and NMR volume at very low SNR. The BRD technique (Figure 5 – panel (b)) produces unimodal distributions at low SNR but bi-modal distributions at SNR of 200 and more while NMR volume never stabilizes.

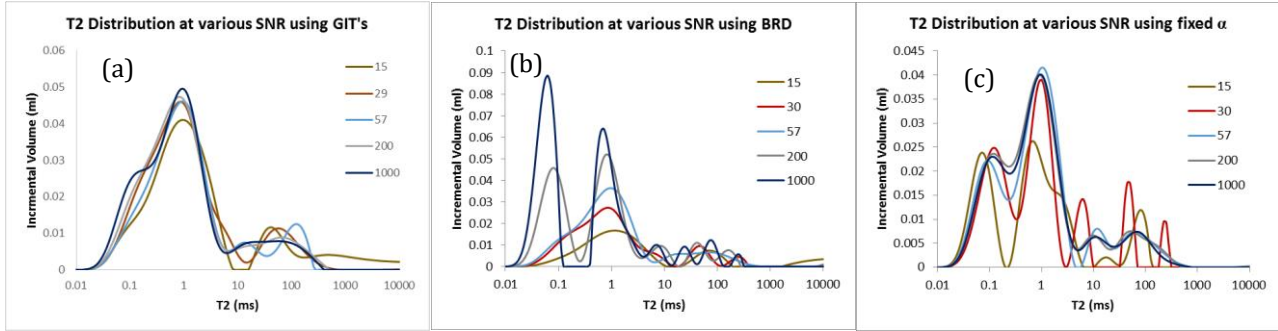


**Figure 5** – T<sub>2</sub> distributions generated using GIT's (a), BRD (b), and Fixed  $\alpha$  (c) techniques at different SNRs. Tests are run at TE=100  $\mu$ s, 10,000 echoes and RD time of 1000 ms.

Depending on the application for the NMR data, accuracy and reliability can be interpreted differently. For example, NMR data is routinely used for permeability predictions. Two prominent models frequently used for permeability prediction from NMR data are the Timur-Coates and SDR models [13]. Timur-Coates correlates permeability to free-to-bound fluid volume ratio while SDR correlates permeability to log-mean relaxation time. T<sub>2</sub> distributions generated at different SNRs using the three smoothing techniques were used to calculate free-to-bound fluid volume ratios as well as log-mean relaxation times. The results are shown in Figure 6. Results indicate that the Fixed  $\alpha$  regularization technique produces stable T<sub>2lm</sub> as well as stable free-to-bound volume even at very low SNR. BRD however, while producing reliable T<sub>2</sub> distributions at high SNR, fails to produce consistent T<sub>2lm</sub> and free-to-bound volumes. GIT's technique fails to produce a bi-modal distribution; however, it outperforms BRD's permeability prediction power at both low and high SNR. In conclusion a fixed smoothing parameter of 0.2 is used for all future inversions in this study.

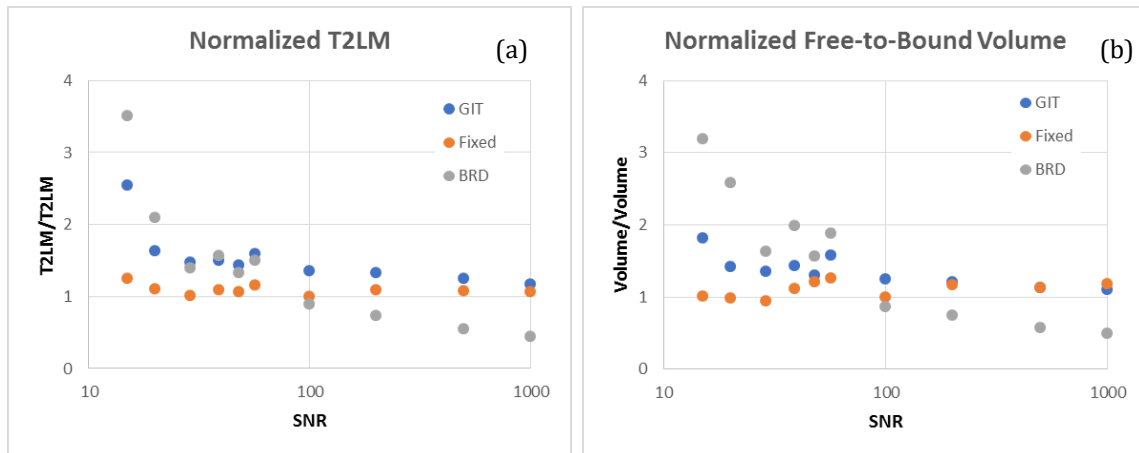


**Figure 6** – A comparison of T<sub>2lm</sub> and Free-to-Bound volumes calculated from T<sub>2</sub> distributions generated using GIT's, BRD and Fixed  $\alpha$  techniques at different SNRs. The results are normalized for T<sub>2lm</sub> and Free-to-Bound volume calculated from T<sub>2</sub> distributions generated using Fixed  $\alpha$  technique at SNR of 100.

## DATA ACQUISITION OPTIMIZATION BACKGROUND SIGNALS

In the laboratory samples are typically put in sample holders or wrapped in Teflon wraps and placed in the spectrometer. As a result there exists the possibility of detecting signal from probe ring down, the holder, wrap or ambient moisture which can be interpreted as signal detected from the rock. In high porosity rocks, the background signal is negligible compared to the main signal coming from the rock; however, in low signal samples such as unconventional rocks, background signals can be very misleading as they can be interpreted as microporosity and result in overestimating the storage capacity of the medium. It is common practice to use digital filters to narrow the frequency range of the signal received from the sample and improve data quality [14]; however, each filtering process imposes an acquisition time delay known as “group delay” [1]. In this study digital filters were used to filter out the background signal. To do so, the holder was placed in the spectrometer and scanned at different echo spacing using different available filters while total NMR signal received by the coil was monitored. To avoid adding noise to the data, the SNR of the background signal was set to match the SNR of the scans that were ran on the sample for other measurements in this study. Initially a 1 MHz filter was used to allow for shorter  $\tau$ s. The 1 MHz filter was able to filter out most of the background signals at  $\tau$  of 70  $\mu$ sec and higher (Figure 7). At lowest  $\tau$ , the signal captured from the holder using the 1MHz filter amounted to double the signal captured from the sample at partially saturated state. The 125 KHz filter however, was able to filter out the entire background signal although the smallest  $\tau$  available on the 125 KHz filter was 50  $\mu$ sec. Therefore the 125 KHz filter was used as the optimum filter for future runs.

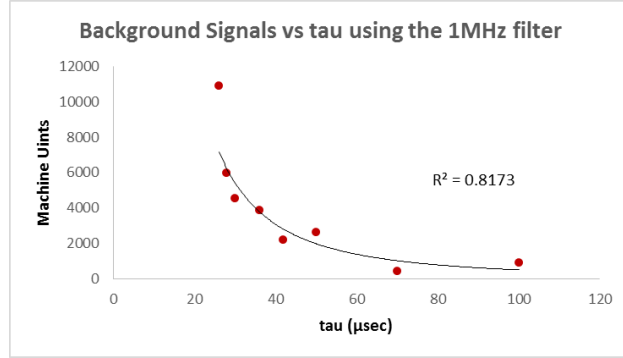


**Figure 7** – Background signal captured from the sample holder at different  $\tau$ s using the 1MHz digital filter

## ECHO SPACING (TE)

The sooner data acquisition starts, i.e. shorter TE, in a CPMG process the more spin echoes are detected [in a given experimental time]. Specifically in fast relaxing unconventional rocks these early time signals play an important role in characterizing heavy hydrocarbons as well as the micro-pore space while rocks with larger pore network and light hydrocarbons are less sensitive to echo spacing. Using the 125 KHz filter, a minimum  $\tau$  of 50  $\mu$ sec could be achieved. The effect of echo spacing on the  $T_2$  distribution curve was studied by running the same test at different echo spacings, ranging from 50  $\mu$ sec to 200  $\mu$ sec in increments of 10  $\mu$ sec. Figure 8 summarizes the results, showing that microporosity (representing fast relaxing atoms) significantly decreases as  $\tau$  is increased and at  $\tau$  of 200  $\mu$ sec 77% of micro-porosity volume is lost and  $T_{2lm}$  increases by 130 percent while meso and macro-porosity volumes are unchanged.

(a)

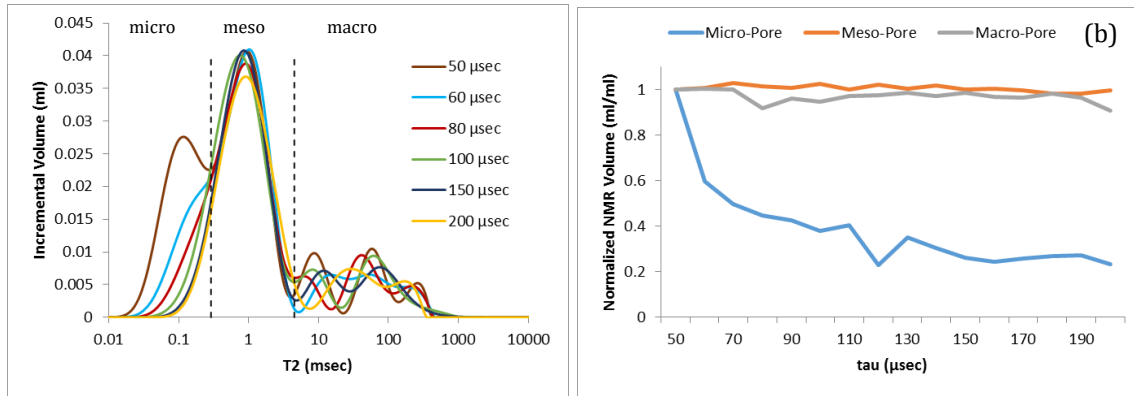


**Figure 8** – A comparison between NMR volumes at different echo spacings, processed using the fixed  $\alpha$  method. Results highlight the fact that at higher echo spacings signal from fast relaxing components of the medium (can be organic porosity or heavy hydrocarbons) is not captured

### NUMBER OF ECHOES

At any given TE, the number of echoes dictates the length of each NMR scan. In unconventional rocks, due to small pore structure and mineralogy, hydrogen nuclei relax faster. Typically scans with a small number of echoes are run to save time, especially during NMR logging operations, dismissing the fact that enough echoes are required to capture all the hydrogen nuclei with different relaxation rates. Acquiring data with an insufficient number of echoes results in discounting the slow relaxing hydrogen nuclei, typically occupying the micro fractures, and underestimating porosity. It is recommended to increase the number of echoes until the echo train data decreases to the noise level.

In this study, the sample is scanned with different numbers of echoes, ranging from 500 to 10,000 echoes. All scans are run at  $\tau=50\mu\text{sec}$  and Repeat-Delay time of 3000 ms. The results (Figure 9) show that at a lower numbers of echoes, 45% of the macro-porosity and 10% of the micro-porosity is not captured. As number of echoes increase, both volumes increase while meso-porosity is unchanged. However, because macro-porosity is a small fraction of the total porosity in this specific sample, total NMR volume is only affected by 10% throughout this analysis.

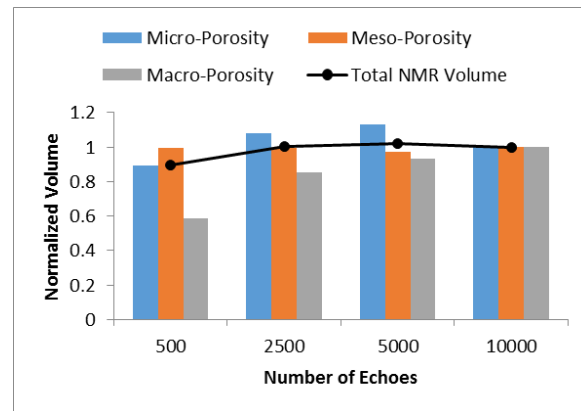


**Figure 9** – Study of susceptibility of NMR volumes to number of echoes. In the presence of larger pores and micro-fractures more echoes (longer scans) are required to capture the signal. Volumes in the graph are normalized for volumes at 10,000 echoes.

### REPEAT-DELAY TIME

Typically, multiple successive CPMG sequences are run to minimize the noise and maximize the signal-to-noise ratio (SNR). Wait times are applied between each successive CPMG sequence to let the spins relax to their equilibrium state. This wait time is referred to as the Repeat-Delay time (RD). In a complex system, where different fluids exist in a complex pore structure of various sizes, RD is typically chosen as 3 to 5 times the largest  $T_1$  relaxation. Choosing too small of a RD time can result in reduction of the total NMR



signal as some atoms will not have returned to their thermal equilibrium when the next CPMG sequence starts.

In this study, a series of RD times, ranging from 100 ms to 3000 ms, were examined on the Montney sample. All these runs were performed at  $\tau=50\mu\text{sec}$ . The results (Figure 10-a) show that up to 30% of the macro-pore NMR volume and up to 20% of the micro-pore NMR volume is lost at lower RD times. Meso-pores, occupied by fast relaxing brine molecules, do not show sensitivity to RD time variations. Micro-pore sensitivity to RD time is either an indication of presence of low viscosity hydrocarbons (such as gases) in the micro-pore space or an indication of the presence of fast relaxing heavy hydrocarbons (such as bitumen) in the pore structure. A  $T_1$ - $T_2$  scan performed on the As-Received sample (Figure 10-b) highlights the presence of high viscosity hydrocarbons in the fast relaxing domain. High viscosity hydrocarbons show higher  $T_1$ - $T_2$  relaxation ratios compared to low viscosity hydrocarbons. As a result, in the presence of heavy hydrocarbons, the  $T_1$ - $T_2$  map will deviate from the 1-1 line. It should be kept in mind that the  $T_1$ - $T_2$  map was obtained from the As-Received sample with residual water saturation.

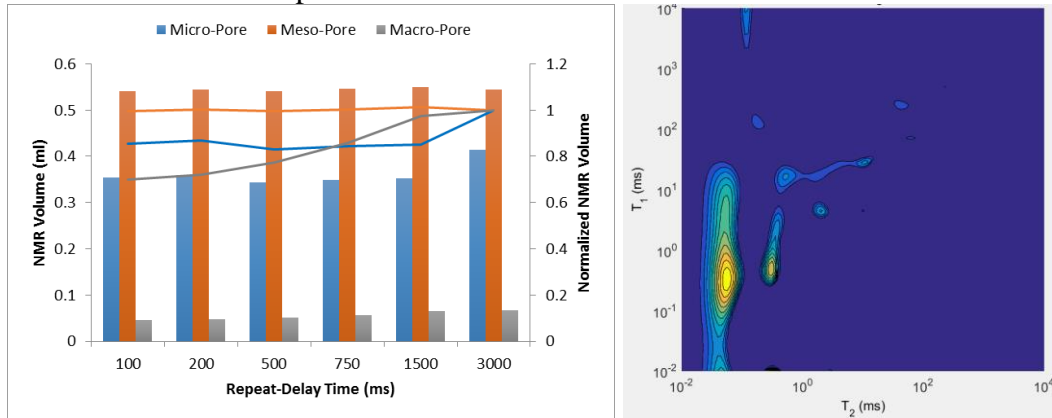


Figure 10 - (a) shows the effect of RD time on NMR volumes while (b) highlights the presence of heavy hydrocarbons in the sample.

## REPEATABILITY OF $T_2$ MEASUREMENTS

On a separate set of samples, an investigation was undertaken into repeatability and error associated with the measurement of  $T_2$  distributions. This data was also used to explore the effect of heating of samples by the rf excitation pulses. All the  $T_2$  relaxation data acquired was fit using the GIT regularization technique.

In the first series of experiments, a calibration sample with a fixed volume of water was used. Its NMR volume was determined repeatedly via 500  $T_2$  measurements (see Table 3 for experimental parameters) done in succession allowing the error in the measurement to be calculated. The series of  $T_2$  measurements was repeated with  $\tau = 100 \mu\text{s}$  and  $500 \mu\text{s}$ . By comparing the  $\tau = 100 \mu\text{s}$  and  $500 \mu\text{s}$  data, the effect of scan sequences with short  $\tau$  and long echo trains versus long  $\tau$  and short echo trains could be examined. The results of the  $T_2$  measurements can be seen in Figure 11, the top panel showing the  $\tau = 500 \mu\text{s}$  data and the bottom panel showing the  $100 \mu\text{s}$  data. Both sets of measurements show a sharp decrease in the NMR volume over the first two to three scans. This is most likely due to heating of the sample during the first few scans. The NMR signal will decrease approximately 0.3% per degree Celsius for temperatures near room temperature. The decrease in signal is not due to a real loss of volume as the sample is sealed. The  $100 \mu\text{s}$  data shows a continual decrease in the NMR volume due to continued heating over the

entire experiment. The same effect is not as pronounced in the 500  $\mu\text{s}$  measurements indicating that heating of the sample is more pronounced for scan sequences with short  $\tau$  and long echo trains.

The measurement error is hard to determine for either set of measurements due to heating of the sample. The best estimate of the error comes from the last fifty measurements in each data set where temperature is most stable and hence having the least effect (i.e.  $\tau = 100 \mu\text{s}$ , measurement error =  $\pm 0.033\%$  and  $\tau = 500 \mu\text{s}$ , measurement error =  $\pm 0.068\%$ ). The lack of shorter  $\tau$  data makes the determination of the NMR volume from the 500  $\mu\text{s}$  data more prone to error leading to a larger measurement error.

In the second series of experiments, a brine saturated sandstone sample was employed. As with the fixed volume sample, its NMR volume was determined repeatedly via 500  $T_2$  measurements done in succession. The rock chosen had a  $T_2$  distribution similar to the fixed volume sample so that the same scan parameters could be employed (see Table 3 for experimental parameters).

Again, a series of  $T_2$  measurements was repeated with  $\tau = 100 \mu\text{s}$  and 500  $\mu\text{s}$ . The results of the  $T_2$  measurements can be seen in Figure 12, the top panel showing the  $\tau = 500 \mu\text{s}$  data and the bottom panel showing the 100  $\mu\text{s}$  data. Neither data set showed heating effects as pronounced as with the fixed volume sample. This indicates that heating of the sample by the rf pulses is not as much of an issue in rock samples as in fixed volume samples.

For rock samples, care must be taken to ensure that any decrease observed is due to heating of the sample and not due to drying as the sandstone was not sealed. From mass measurements before and after the NMR experiments, it was determined that the rock loses about 0.1 ml/hour of brine due to drying. Removing this drying rate from the NMR data, it is determined that for the  $\tau = 500 \mu\text{s}$  data the entire change in volume over the experimental time is due to drying, while some of the volume change in the  $\tau = 100 \mu\text{s}$  data is due to heating.

**Table 3** – Experimental Parameters for Fixed Volume and sandstone samples

Sample	Fixed Volume Sample	Fixed Volume Sample	Sandstone Sample	Sandstone Sample
Expected Volume	20.75 ml	20.75 ml	12.4 ml	12.4 ml
Number of Scans	16	16	16	16
Number of Echoes	2500	500	2500	500
Recycle Delay	750 ms	750 ms	750 ms	750 ms
Filter	125 KHz	125 KHz	125 KHz	125 KHz
$T_2$ Max	100 ms	100 ms	100 ms	100 ms
$\tau$	100 $\mu\text{s}$	500 $\mu\text{s}$	100 $\mu\text{s}$	500 $\mu\text{s}$
Approx. SNR	450	450	250	220

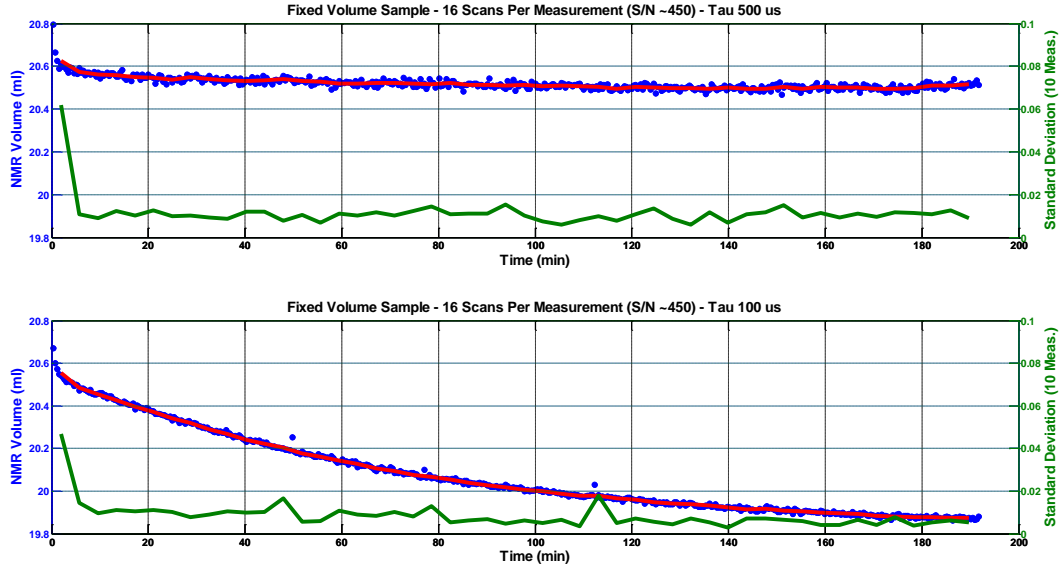


**Figure 11** -  $T_2$  volume measurements for a fixed volume sample versus time at two different echo spacings. The graph shows that at smaller  $\tau$  heating effects are more severe and lead to major variations in NMR volume

The measurement error is hard to determine for either set of measurements due to the temperature/drying effects observed in the rocks. The best estimate comes from the last fifty measurements in each data set where temperature is most stable and hence having the least effect (i.e.  $\tau = 100 \mu\text{s}$ , measurement error =  $\pm 0.304\%$  and  $\tau = 500 \mu\text{s}$ , measurement error =  $\pm 0.596\%$ ). The lack of shorter  $\tau$  data makes the determination of the NMR volume from the  $500 \mu\text{s}$  data more prone to error leading to a larger measurement error.

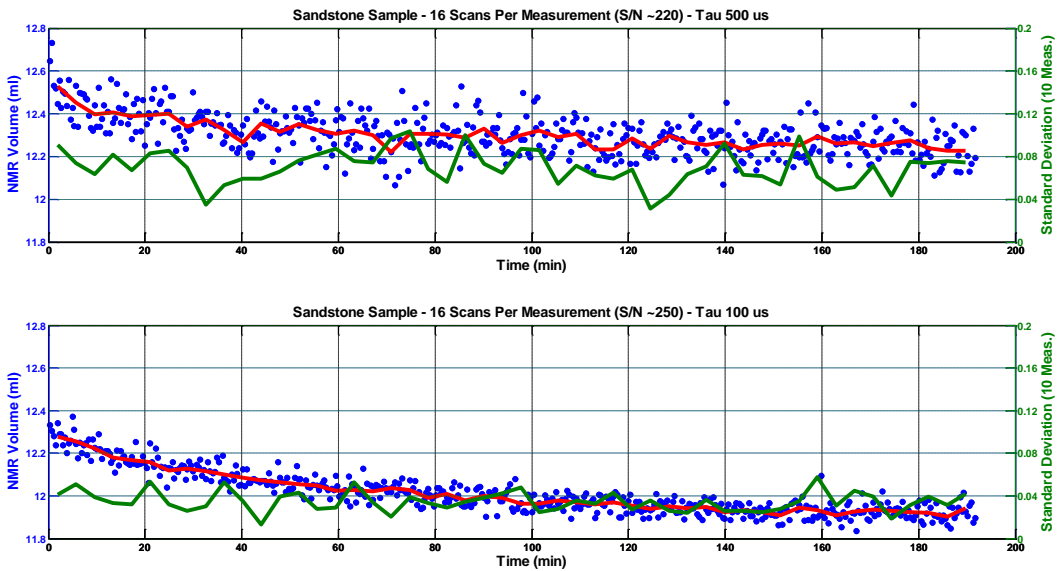


**Figure 12** -  $T_2$  volume measurements for a sandstone sample versus time at two different echo spacings. The graph shows that at smaller  $\tau$  drying effects are more severe and lead to major variations in NMR volume

## CONCLUSIONS

This study was performed on a tight rock sample to analyze the challenges imposed on NMR data acquisition and analysis due to the presence of fast relaxing hydrogen atoms in the pore space of such rocks. Factors such as smoothing parameter, echo spacing, repeat-delay times, background signals, number of echoes, and repeatability of the measurements were examined. In this study we were able to show that

- Due to the fast relaxation of the hydrogen nuclei in unconventional rocks, NMR data inversion is more challenging in these rocks compared to conventional rocks. A Fixed  $\alpha$  inversion technique was compared with other available techniques and proved to be capable of producing reliable and consistent  $T_2$  distributions even at low SNR. It should be noted that the Fixed  $\alpha$  was achieved in a lab setting by scanning the sample at two saturation levels. In the field or where scanning samples at various saturation levels is not possible, it is still recommended to run an initial scan with high SNR and calculate  $\alpha$  using a trusted inversion technique and use the same  $\alpha$  at lower SNR to save time to achieve reliable results.
- A 125KHz digital filter proved to be able to eliminate the entire background signal. Although it was possible to run shorter echo spacings, as small as 26  $\mu\text{s}$ , with the 1MHz filter, the filter could remove the majority of the background signal only at  $\tau=70 \mu\text{s}$  and larger.
- Short echo spacing, with a large number of echoes should be used to capture all the signal from the micro-pore space to the micro-fractures. Long Repeat-Delay times should be used to let all atoms relax to their thermal equilibrium before the commencement of the next re-phasing. Using short RD times would result in the loss of signal specially from heavy hydrocarbons as well as the macro-pore space.
- Heating and drying effects should be accounted for when consecutive NMR measurements are performed on samples. Particularly at short echo spacings heating/drying effects are more significant and can lead to discrepancies.

## REFERENCES

- [1] Saidian, M., and M. Prasad. "Nuclear Magnetic Resonance (NMR) Measurements for Mudrock (Shale) Characterizations: Challenges in Data Acquisition and Signal Processing" *Journal of Magnetic Resonance*, Submitted (2015)
- [2] Kenyon, W. E., 1992, "Nuclear magnetic resonance as a petrophysical measurement", *Nuclear Geophysics*, v. 6, no. 2, p. 153-171.
- [3] Saidian, M., "A comparison of measurement techniques for porosity and pore size distribution in mudrocks: a case study of Haynesville, Niobrara, Monterey and Eastern European Silurian Formations." *AAPG Memoir* 110 (2015): 60
- [4] Passey, Q. R., K. M. Bohacs, W. L. Esch, R. Klimentidis and S. Sinha, 2010, "From oil-prone source rock to gas-producing shale reservoir—geologic and petrophysical characterization of unconventional shale-gas reservoirs" *International Oil and Gas Conference and Exhibition*, SPE Paper 131350
- [5] Chalmers G. and R. Bustin, "Geological Evaluation of Halfway–Doig–Montney Hybrid Gas Shale–Tight Gas Reservoir, Northeastern British Columbia," *Marine and Petroleum Geology*, vol. 38, no. 1, pp. 53-72, 2012
- [6] Wüst R. A., B. R. Nassichuk and R. M. Bustin, "Porosity Characterization of Various Organic-rich Shales from the Western Canadian Sedimentary Basin, Alberta and

- British Columbia, Canada," *M102-Electron Microscopy of Shale Hydrocarbon Reservoirs, American Association of Petroleum Geologists*, 2013, pp. 81-100
- [7] Ghanizadeh A., S. Aquinto, C. R. Clarkson, O. Haeri-Ardakani and H. Sanei, "Petrophysical and Geomechanical Characteristics of Canadian Tight Oil and Liquid-Rich Gas Reservoirs," *SPE/CSUR Unconventional Resources Conference*, Calgary, Alberta, Sep 30 - Oct 2, 2014.
- [8] Meiboom, S., and D. Gill, 1958, "Modified Spin - Echo Method for Measuring Nuclear Relaxation Times," *Review of Scientific Instrument*, Vol. 29, No. 8, P. 668-691
- [9] Carr, H., and E. Purcell, 1954, "Nuclear magnetic resonance: Petrophysical and logging applications," *Physical Review*, v. 94, No. 3, P. 630-638
- [10] Coates, G. R., X. Lizhei, and M. G. Prammer, *NMR Logging Principles and Applications*, Haliburton Energy Services Publication, 1999
- [11] Dunn K. J., D. J. Bergman and G. A. LaTorraca, *Nuclear Magnetic Resonance: Petrophysical and Logging Applications*, Elsevier, 2002
- [12] Song, Y-Q., et al. "T1-T2 correlation spectra obtained using a fast two-dimensional Laplace inversion." *Journal of Magnetic Resonance* 154.2 (2002): 261-268.
- [13] Salimifard B., D. W. Ruth, D. Green and D. Veselinovic, "Developing a Model to Estimate Permeability from Other Petrophysical Data," *International Symposium of the Society of Core Analysts*, Avignon, France, 2014
- [14] Moskau, D., 2001, "Application of Real Time Digital Filters in NMR Spectroscopy, Concepts," *Magnetic Resonance*, v. 15, no. 2, p. 164-176